

# A Laser Flash Photolysis and Quantum Chemical Study of the Fluorinated Derivatives of Singlet Phenylnitrene

Nina P. Gritsan,<sup>\*,†</sup> Anna Dóra Gudmundsdóttir,<sup>‡</sup> Dean Tigelaar,<sup>‡</sup> Zhendong Zhu,<sup>‡</sup>  
William L. Karney,<sup>\*,§</sup> Christopher M. Hadad,<sup>\*,‡</sup> and Matthew S. Platz<sup>\*,‡</sup>

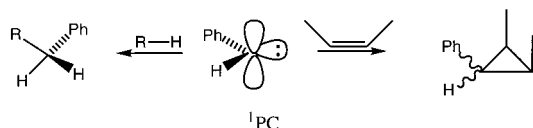
Contribution from the Institute of Chemical Kinetics and Combustion and Novosibirsk State University, 630090 Novosibirsk, Russia, Newman and Wolfrom Laboratory of Chemistry, The Ohio State University, 100 West 18th Avenue, Columbus, Ohio 43210, and Department of Chemistry, University of San Francisco, 2130 Fulton Street, San Francisco, California 94117-1080

Received December 20, 1999. Revised Manuscript Received December 6, 2000

**Abstract:** Laser flash photolysis (LFP, Nd:YAG laser, 35 ps, 266 nm, 10 mJ or KrF excimer laser, 10 ns, 249 nm, 50 mJ) of 2-fluoro-, 4-fluoro-, 3,5-difluoro-, 2,6-difluoro-, and 2,3,4,5,6-pentafluorophenyl azides produces the corresponding singlet nitrenes. The singlet nitrenes were detected by transient absorption spectroscopy, and their spectra are characterized by sharp absorption bands with maxima in the range of 300–365 nm. The kinetics of their decay were analyzed as a function of temperature to yield observed decay rate constants,  $k_{\text{OBS}}$ . The observed rate constant in inert solvents is the sum of  $k_{\text{R}} + k_{\text{ISC}}$  where  $k_{\text{R}}$  is the absolute rate constant of rearrangement of singlet nitrene to an azirine and  $k_{\text{ISC}}$  is the absolute rate constant of nitrene intersystem crossing (ISC). Values of  $k_{\text{R}}$  and  $k_{\text{ISC}}$  were deduced after assuming that  $k_{\text{ISC}}$  is independent of temperature. Barriers to cyclization of 4-fluoro-, 3,5-difluoro-, 2-fluoro-, 2,6-difluoro-, and 2,3,4,5,6-pentafluorophenyl nitrene in inert solvents are  $5.3 \pm 0.3$ ,  $5.5 \pm 0.3$ ,  $6.7 \pm 0.3$ ,  $8.0 \pm 1.5$ , and  $8.8 \pm 0.4$  kcal/mol, respectively. The barrier to cyclization of parent singlet phenyl nitrene is  $5.6 \pm 0.3$  kcal/mol. All of these values are in good quantitative agreement with CASPT2 calculations of the relative barrier heights for the conversion of fluoro-substituted singlet aryl nitrenes to benzazirines (Karney, W. L. and Borden, W. T. *J. Am. Chem. Soc.* **1997**, *119*, 3347). A single *ortho*-fluorine substituent exerts a small but significant bystander effect on remote cyclization that is not steric in origin. The influence of two *ortho*-fluorine substituents on the cyclization is pronounced. In the case of the singlet 2-fluorophenyl nitrene system, evidence is presented that the benzazirine is an intermediate and that the corresponding singlet nitrene and benzazirine interconvert. Ab initio calculations at different levels of theory on a series of benzazirines, their isomeric ketenimines, and the transition states converting the benzazirines to ketenimines were performed. The computational results are in good qualitative and quantitative agreement with the experimental findings.

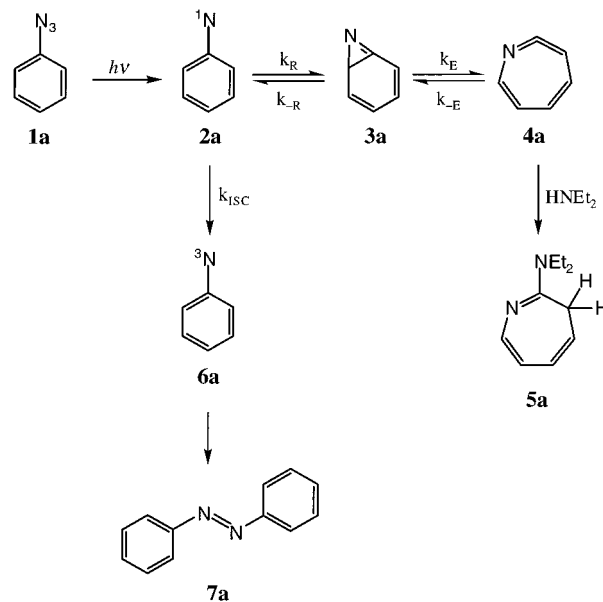
## I. Introduction

Singlet phenylcarbene (<sup>1</sup>PC) reacts with a variety of reagents to form adducts in good yield.<sup>1</sup>



Singlet phenylnitrene (**2a**) does not react with alkenes and alkanes to form adducts as efficiently as does singlet phenylcarbene (<sup>1</sup>PC).<sup>2</sup> Photolysis of phenyl azide (**1a**) releases singlet phenyl nitrene (**2a**), which isomerizes to benzazirine (**3a**, Scheme 1) more rapidly than it undergoes bimolecular reactions at ambient temperature. Benzazirine **3a** can be intercepted with ethanethiol before it opens to form cyclic ketenimine (didehydroazepine) **4a**.<sup>3</sup> This species can be intercepted with diethyl-

## Scheme 1



amine to form an azepine adduct (**5a**).<sup>4</sup> In the absence of amine nucleophiles the ketenimine reverts slowly to singlet phenyl nitrene and relaxes to triplet phenyl nitrene under conditions of

<sup>†</sup> Institute of Chemical Kinetics and Combustion and Novosibirsk State University.

<sup>‡</sup> The Ohio State University.

<sup>§</sup> University of San Francisco.

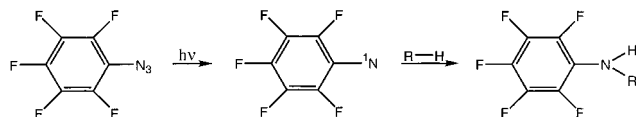
(1) For a review see Baron, W. J.; DeCamp, M. R.; Henrick, M. E.; Jones, M., Jr.; Levin, R. H.; Sohn, M. B. In *Carbenes*; Jones, M., Jr., Moss, R. A., Eds.; Wiley: New York, 1973; Vol. I. p 1.

(2) Schuster, G. B.; Platz, M. S. *Adv. Photochem.* **1992**, *17*, 69.

high dilution.<sup>5</sup> In solutions of moderate concentration, ketenimine **4a** reacts with phenyl azide to form a polymeric tar.<sup>6</sup>

As mentioned previously, singlet phenylnitrene rearranges in solution at ambient temperature to benzazirine. The rate of this process decreases as the temperature decreases. At ~180 K the rate constant for rearrangement ( $k_R$ ) of singlet phenylnitrene equals the rate constant for intersystem crossing ( $k_R = k_{ISC}$ , Scheme 1),<sup>7</sup> which is independent of temperature.<sup>8</sup> Thus, below 180 K, triplet phenylnitrene (**6a**) is irreversibly formed in solution, and it eventually dimerizes to form azobenzene (**7a**).<sup>7,8</sup>

In separate experiments the Abramovitch group<sup>9</sup> and Banks and co-workers<sup>10</sup> demonstrated that polyfluorinated singlet nitrenes have rich and useful bimolecular chemistry. The original observations were extended by the Keana group<sup>11</sup> and this laboratory.<sup>12</sup> Polyfluorinated singlet aryl nitrenes insert into the C–H bonds of hydrocarbons (R–H) but do not react with methylene chloride or Freon solvents.<sup>12</sup> C–H insertion chemistry is observed when fluorine atom substituents occupy both positions *ortho* to the nitrene center, but this reaction has not been reported for other types of fluorinated aryl nitrenes.<sup>2</sup>

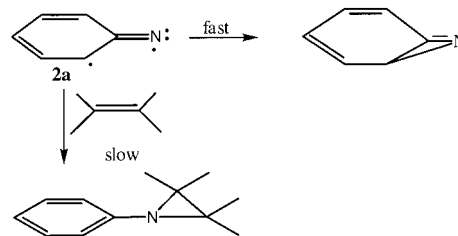


The isokinetic temperature, where  $k_R = k_{ISC}$ , is near 270 K for singlet perfluorophenylnitrene.<sup>12</sup>

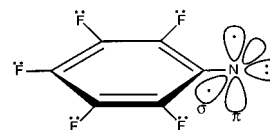
Platz,<sup>12</sup> Keana,<sup>11</sup> and Bayley<sup>13</sup> have predicted that polyfluorinated aryl azides might be useful as photoaffinity labeling reagents, which has prompted several comparative studies of fluorinated and nonfluorinated aryl nitrenes.<sup>14</sup>

<sup>1</sup>PC reacts rapidly with bonding and nonbonding pairs of electrons through initial coordination of the empty p orbital of

the carbene.<sup>1,15</sup> Although <sup>1</sup>PC has a closed-shell electronic structure,<sup>16</sup> calculations<sup>17,18</sup> and experiments<sup>19</sup> indicate that singlet phenylnitrene has an open-shell electronic structure and is 18.5 kcal/mol higher in energy than triplet phenylnitrene. The diradical **2a** cannot smoothly undergo concerted cycloaddition reactions with alkenes to form azirines.<sup>20</sup>



We have postulated that the fluorine substituents exert an electronic effect which makes the  $\pi^2$  configuration more accessible by  $\pi$ -back-bonding.<sup>12</sup> Fluorine substituents make the nitrene look like a carbene from this perspective, which explains the heightened bimolecular chemistry of polyfluorinated aryl nitrenes.<sup>20</sup>



Although this view has received support from the density functional theory (DFT) calculations of Smith and Cramer,<sup>21</sup> a different interpretation has been offered by Karney and Borden using the CASPT2 method.<sup>22</sup> These latter calculations indicate that *ortho*-fluorine substituents raise the barrier for cyclization to the corresponding azirine by 3.5–4.5 kcal/mol, relative to parent **2a**, through a combination of steric and electronic factors.<sup>22</sup>

Two groups have recently reported the direct spectroscopic detection of **2a** by laser flash photolysis.<sup>23,24</sup> Singlet phenylnitrene has a sharp absorption band at 350 nm. The lifetime of

(3) Carroll, S. E.; Nay, B.; Scriven, E. F. V.; Suschitzky, H.; Thomas, D. R. *Tetrahedron Lett.* **1977**, 3175.

(4) (a) Doering, W. v. E.; Odum, R. A. *Tetrahedron* **1966**, 22, 81. (b) DeGruff, B. A.; Gillespie, D. W.; Sundberg, R. J. *J. Am. Chem. Soc.* **1974**, 96, 7491.

(5) (a) Gritsan, N. P.; Pritchina, E. A. *J. Inf. Rec. Mater.* **1989**, 17, 391. (b) Gritsan, N. P.; Pritchina, E. A. *Russ. Chem. Rev.* **1992**, 61, 500. (c) Li, Y.-Z.; Kirby, J. P.; George, M. W.; Poliakoff, M.; Schuster, G. B. *J. Am. Chem. Soc.* **1988**, 110, 8092. (d) Schrock, A. K.; Schuster, G. B. *J. Am. Chem. Soc.* **1984**, 106, 715. (e) Younger, C. G.; Bell, R. A. *J. Chem. Soc., Chem. Commun.* **1982**, 1359.

(6) Meijer, E. W.; Nijhuis, S.; Von Vroonhoven, F. C. B. M. *J. Am. Chem. Soc.* **1988**, 110, 7209.

(7) Leyva, E.; Platz, M. S.; Persy, G.; Wirz, J. *J. Am. Chem. Soc.* **1986**, 108, 3783.

(8) Gritsan, N. P.; Hadad, C. M.; Zhu, Z.; Platz, M. S. *J. Am. Chem. Soc.* **1999**, 121, 1202.

(9) (a) Abramovitch, R. A.; Challand, S. R.; Scriven, E. F. V. *J. Am. Chem. Soc.* **1972**, 94, 1374. (b) Abramovitch, R. A.; Challand, S. R.; Scriven, E. F. V. *J. Org. Chem.* **1975**, 40, 1541.

(10) (a) Banks, R. E.; Sparkes, G. R. *J. Chem. Soc., Perkin Trans. 1* **1972**, 1964. (b) Banks, R. E.; Venayak, N. D. *J. Chem. Soc., Chem. Commun.* **1980**, 900. (c) Banks, R. E.; Prakash, A. *Tetrahedron Lett.* **1973**, 99. (d) Banks, R. E.; Prakash, A. *J. Chem. Soc., Perkin Trans. 1* **1974**, 1365. (e) Banks, R. E.; Madany, I. M. *J. Fluorine Chem.* **1985**, 30, 211.

(11) (a) Keana, J. F. W.; Cai, S. X. *J. Fluorine Chem.* **1989**, 43, 151. (b) Keana, J. F. W.; Cai, S. X. *J. Org. Chem.* **1990**, 55, 2034. (c) Cai, S. X.; Keana, J. F. W. *Bioconjugate Chem.* **1991**, 2, 28. (d) Cai, S. X.; Glenn, D. R.; Keana, J. F. W. *J. Org. Chem.* **1992**, 57, 1299.

(12) (a) Poe, R.; Schnapp, K.; Young, M. J. T.; Grayzar, J.; Platz, M. S. *J. Am. Chem. Soc.* **1992**, 114, 5054. (b) Young, M. J. T.; Platz, M. S. *J. Org. Chem.* **1991**, 56, 6403. (c) Marcinek, A.; Platz, M. S. *J. Phys. Chem.* **1993**, 97, 12674. (d) Marcinek, A.; Platz, M. S.; Chen, S. Y.; Floresco, R.; Rajagopalan, K.; Golinsk, M.; Watt, D. *J. Phys. Chem.* **1994**, 98, 412. (e) Schnapp, K.; Platz, M. S. *Bioconjugate Chem.* **1993**, 4, 178. (f) Schnapp, K.; Poe, R.; Leyva, E.; Soundararajan, N.; Platz, M. S. *Bioconjugate Chem.* **1993**, 4, 172.

(13) Bayley, H. *Photogenerated Reagents in Biochemistry and Molecular Biology*; Elsevier: Amsterdam, 1983.

(14) (a) Crocker, P. J.; Imai, N.; Rajagopalan, K.; Bogges, M. A.; Kwiatkowski, S.; Dwyer, L. D.; Vanaman, T. C.; Watt, D. S. *Bioconjugate Chem.* **1990**, 1, 419. (b) Drake, R. R.; Slama, J. T.; Wall, K. A.; Abramova, M.; D'Souza, C.; Elbein, A. D.; Crocker, P. J.; Watt, D. S. *Bioconjugate Chem.* **1992**, 3, 69. (c) Pinney, K. C.; Katzenellenbogen, J. A. *J. Org. Chem.* **1991**, 56, 3125. (d) Pinney, K. C.; Carlson, K. E.; Katzenellenbogen, S. B.; Katzenellenbogen, J. A. *Biochemistry* **1991**, 30, 2421. (e) Reed, M. W.; Fraga, D.; Schwarts, D. E.; Scholler, J.; Hinrichsen, R. D. *Bioconjugate Chem.* **1995**, 6, 101. (f) Kapfer, I.; Jacques, P.; Toubal, H.; Goeldner, M. P. *Bioconjugate Chem.* **1995**, 6, 109. (g) Kym, P. R.; Carlson, K. E.; Katzenellenbogen, J. A. *J. Med. Chem.* **1993**, 36, 1993. (h) Kapfer, I.; Hawkinson, J. E.; Casida, J. E.; Goeldner, M. P. *J. Med. Chem.* **1994**, 37, 133.

(15) Hoffman, R.; Zeiss, G. D.; Van Dine, G. W. *J. Am. Chem. Soc.* **1968**, 90, 1485.

(16) (a) Matzinger, S.; Bally, T.; Patterson, E. V.; McMahon, R. J. *J. Am. Chem. Soc.* **1996**, 118, 1535. (b) Wong, M. W.; Wentrup, C. *J. Org. Chem.* **1996**, 61, 7022. (c) Schreiner, P. R.; Karney, W. L.; Schleyer, P. v. R.; Borden, W. T.; Hamilton, T. P.; Schaefer, H. F., III. *J. Org. Chem.* **1996**, 61, 7030.

(17) Kim, S.-J. I.; Hamilton, T. P.; Schaefer, H. F., III. *J. Am. Chem. Soc.* **1992**, 114, 5349.

(18) Hrovat, D. A.; Waali, E. E.; Borden, W. T. *J. Am. Chem. Soc.* **1992**, 114, 8698.

(19) Travers, M. J.; Cowles, D. C.; Clifford, E. P.; Ellison, G. B. *J. Am. Chem. Soc.* **1992**, 114, 8699.

(20) Platz, M. S. *Acc. Chem. Res.* **1995**, 28, 487.

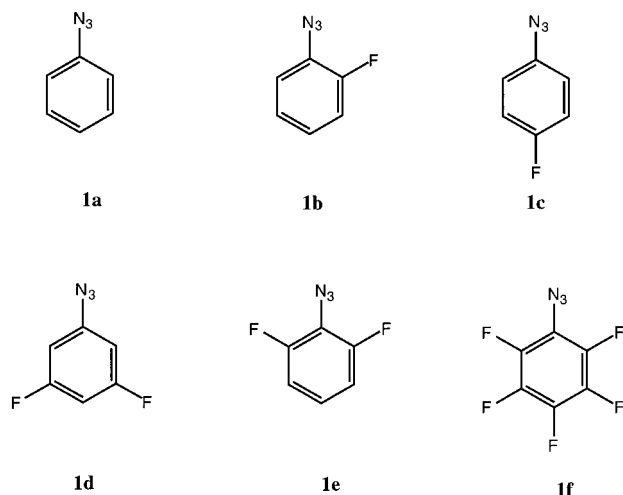
(21) Smith, B. A.; Cramer, C. J. *J. Am. Chem. Soc.* **1996**, 118, 5490.

(22) Karney, W. L.; Borden, W. T. *J. Am. Chem. Soc.* **1997**, 119, 3347.

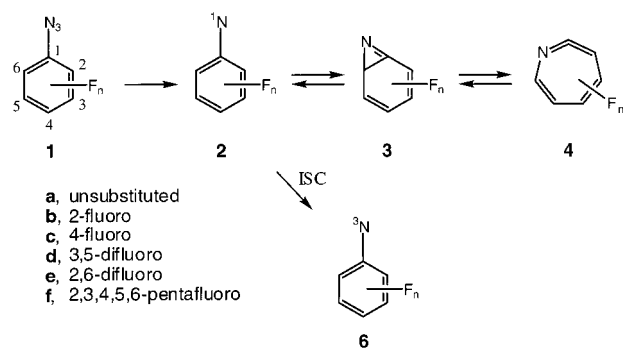
(23) Gritsan, N. P.; Yuzawa, T.; Platz, M. S. *J. Am. Chem. Soc.* **1997**, 119, 5059.

(24) Born, R.; Burda, C.; Senn, P.; Wirz, J. *J. Am. Chem. Soc.* **1997**, 119, 5061.

## Scheme 2



## Scheme 3



**2a** in pentane at 25 °C is about 1 ns. The activation barrier to its rearrangement was first reported to be 6.2 kcal/mol.<sup>23</sup> However, more recent studies place the barrier at  $5.6 \pm 0.3$  kcal/mol,<sup>8</sup> in excellent agreement with theory.<sup>25</sup>

The present study was undertaken to better understand the fluorine effect and to test the predictions of theory<sup>22</sup> in this regard. Thus, 2-fluoro- (**1b**), 4-fluoro- (**1c**), 3,5-difluoro- (**1d**), and 2,6-difluoro- (**1e**) phenyl azides were synthesized (Scheme 2), and the corresponding singlet (**2b–2e**) and triplet (**6b–6e**) nitrenes, azirines (**3b–3e**) (Scheme 3), and ketenimines (**4b–4e**) were studied by laser flash photolysis (LFP). Perfluorophenyl azide (**1f**) has been studied previously,<sup>26</sup> and the LFP data obtained with the corresponding singlet nitrene (**2f**) is included here for convenience. To understand the unique kinetic data for 2-fluorophenyl nitrene and to probe the energetics of the second step of the ring expansion, quantum chemical calculations were performed on these species as well.

## II. Results

The results obtained with 2,6-difluorophenyl azide (**1e**) are representative. LFP of **1e** releases singlet nitrene **2e**, which exhibits an absorption spectrum characterized by two maxima at 324 and 340 nm, similar to that of singlet phenyl nitrene (**2a**).<sup>8</sup> The spectrum of the singlet nitrene was recorded immediately after the laser pulse with an optical multichannel analyzer at 195 K (Figure 1, spectrum 1). The spectrum recorded 1.5  $\mu$ s after the laser pulse (Figure 1, spectrum 2) is attributed to the corresponding triplet nitrene **6e** and is in agreement with the

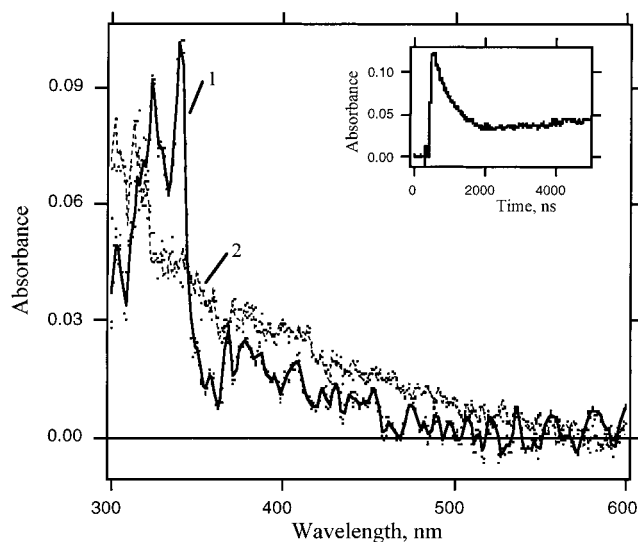


**Figure 1.** The transient absorption spectra produced upon LFP (249 nm) of 2,6-difluorophenyl azide (**1e**) in pentane at 195 K. Spectrum 1 was recorded over a window of 100 ns immediately after the laser pulse. Spectrum 2 was recorded 1.5  $\mu$ s after the laser pulse and is of mainly triplet nitrene **6e**. Inset: the decay kinetics of singlet nitrene **2e** at 195 K monitored at 340 nm.

spectrum of the same nitrene observed as a persistent species in low-temperature matrixes.<sup>7,27</sup> The sensitivity and resolution of the matrix spectrum<sup>7,27</sup> are superior to that in solution, but the sharp band at  $\lambda_{\text{max}} = 310$  nm is clearly discerned in solution phase.

Figure 2 reveals the decay of singlet 2,6-difluorophenyl nitrene (**2e**) (340 nm) and the growth of ketenimine **4e** and triplet nitrene **6e** (380 nm). A slow growth of transient absorption was observed on the microsecond time scale (Figure 1, insert; Figure 2A) due to the dimerization of triplet nitrenes to form azobenzenes,<sup>7</sup> which absorb strongly in the UV region (Supporting Information). The rate of formation of **4e** is the same as the rate of disappearance of **2e**. If there is a benzazirine intermediate (**3e**) in this transformation, as predicted by theory,<sup>22,25</sup> it must open to the corresponding ketenimine at a rate that is much faster than the rate at which it is formed ( $k_E \gg k_R$ , Scheme 1). This was true for parent phenyl nitrene<sup>8,23</sup> and all of the nitrenes included in this study, over the entire temperature range studied, with the notable exception of 2-fluorophenyl nitrene (**2b**) (vide infra).

Singlet nitrene **2e** decays in an exponential process (Figure 2A) which can be analyzed to yield an observed rate constant  $k_{\text{OBS}}$ . Triplet nitrene dimerization forms an azobenzene whose absorption at 340 nm results in the appearance of a slow growth in absorbance at this wavelength (see Supporting Information). This process was explicitly considered in the analysis of the decay kinetics. Values of  $k_{\text{OBS}}$  were measured as a function of temperature (Figure 3). The magnitude of  $k_{\text{OBS}}$  decreases as the temperature is reduced but then reaches a constant value around 270 K. Similar results were obtained with singlet 2-fluorophenyl nitrene (**2b**) and the other singlet nitrenes of this work (Scheme 3), but the onset of the temperature-independent region of  $k_{\text{OBS}}$  varied with the structure of the nitrene.

The temperature-independent value of  $k_{\text{OBS}}$ , measured at low temperatures, is equated with  $k_{\text{ISC}}$ . If  $k_{\text{ISC}}$  is independent of temperature, then values of  $k_R$  can be deduced ( $k_R = k_{\text{OBS}} - k_{\text{ISC}}$ ) along with its associated Arrhenius parameters (Figure 4, Table 1). For the determination of  $k_R$  for 2-fluorophenyl nitrene

(25) Karney, W. L.; Borden, W. T. *J. Am. Chem. Soc.* **1997**, *119*, 1378.

(26) Gritsan, N. P.; Zhai, H. B.; Yuzawa, T.; Karweik, D.; Brooke, J.; Platz, M. S. *J. Phys. Chem. A* **1997**, *101*, 2833.

(27) Morawietz, J.; Sander, W. *J. Org. Chem.* **1996**, *61*, 4351.

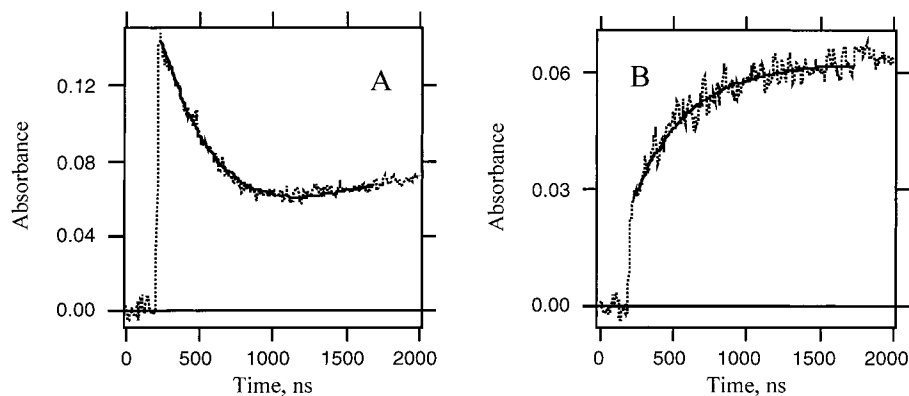


**Figure 2.** The disappearance of singlet nitrene **2e** (A, 340 nm) and the formation of ketenimine **4e** and triplet nitrene **6e** (B, 380 nm) following LFP (249 nm) of 2,6-difluorophenyl azide **1e** in pentane at 295 K.

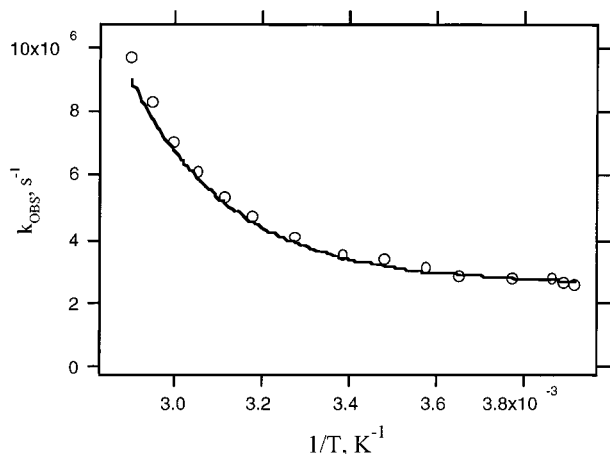


**Figure 3.** Values of  $k_{OBS}$  of singlet nitrene **2e** as a function of temperature in  $CCl_4$  obtained by LFP (249 nm).

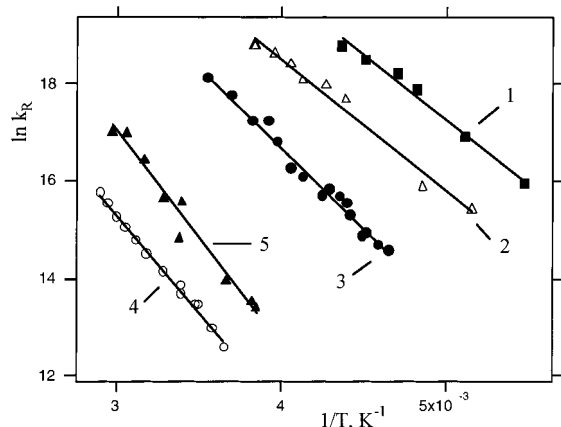


**Figure 4.** Arrhenius treatment of  $k_R (= k_{OBS} - k_{ISC})$  for singlet fluorophenylnitrenes **2c** (1), **2d** (2) in pentane and **2e** (4) in  $CCl_4$  and  $k_R$  for singlet 2-fluorophenylnitrene **2b** (3) calculated as described in the text. (5) Arrhenius treatment of the rate constant of ring-opening reaction ( $k_E$ ) for benzazirine **3b**.

(**2b**), a more complicated procedure was used, which will be described in the next section.

**LFP of 2-Fluorophenyl Azide 1b.** In the case of short-lived singlet nitrenes ( $\tau < 100$  ns), transient spectra were obtained by measuring transient absorption, point-by-point, 2 ns after the laser flash. This is illustrated in Figure 5 for singlet 2-fluorophenylnitrene **2b**. The spectrum of singlet nitrene **2b** is similar to the spectra of singlet 2,6-difluorophenylnitrene (**2e**) (Figure 1, spectrum 1) and parent singlet phenylnitrene **2a**.<sup>8,23</sup>

Unique kinetic results were obtained upon LFP of azide **1b**. Figure 6 displays the typical kinetics of the decay of singlet 2-fluorophenylnitrene (**2b**) and the formation of products (ketenimine **4b** and triplet nitrene **6b**) at different temperatures. All other substituted singlet phenylnitrenes studied in this work and previously<sup>23,26,33</sup> exhibited rates of nitrene decay that were equal to the rates of product formation. At low temperatures where triplet nitrenes are formed in higher yields, slow growths in absorption similar to those displayed in Figure 6G were observed on microsecond time scales due to triplet nitrene dimerization to form azobenzenes which absorb in the UV region.<sup>7</sup>

When the characteristic time constants of nitrene **2b** decay and azepine **4b** and triplet nitrene **6b** growth are significantly different ( $\geq 10$  times), the kinetics of decay (Figure 6A, C, E) and growth (Figure 6B, D, F) can be fitted to exponential functions. These kinetics were analyzed to yield the observed rate constants of decay ( $k_{dec}$ ) and growth ( $k_{gr}$ ). In the general case (vide infra), the kinetics should be analyzed as biexponential (See Supporting Information, Figure S1 and related discussion). In addition, the process of triplet nitrene dimerization was considered in the analysis of decay kinetics at low temperatures (Figure 6G) (See Supporting Information).

It will be assumed that fluorobenzazirine **3b** has no significant absorption above 350 nm. In support of this assumption we note that matrix-isolated difluorobenzazirine **3e** has  $\lambda_{max} = 280$  nm.<sup>27</sup> Furthermore, our CIS/6-31G\* calculations<sup>28</sup> of the spectrum of **3b** yield the following transitions:  $\lambda_{max}(f) = 273$  nm (0.013), 242 nm (0.053), 198 nm (0.116).

Figure 7 presents the temperature dependence of  $k_{dec}$  and  $k_{gr}$ . Figures 6 and 7 reveal that the decay of singlet nitrene **2b** is much faster than the formation of products (**4b** and **6b**) at temperatures above 230 K. Between 147 and 180 K, however,  $k_{gr}$  is equal to  $k_{dec}$  and both rate constants are temperature-independent. In this temperature range (147–180 K), **2b** cleanly relaxes to the lower energy triplet nitrene **6b**.

Above 180 K, **2b** decays by both intersystem crossing ( $k_{ISC}$ ) and cyclization ( $k_R$ ), with the latter process gaining relative to the former as the temperature increases. We will demonstrate that the data of Figure 7 can be explained by positing that singlet

(28) Foresman, J. B.; Head-Gordon, M.; Pople, J. A.; Frisch, M. J. *J. Phys. Chem.* **1992**, *96*, 135.

(29) Andersson, K. *Theor. Chim. Acta* **1995**, *91*, 31.

(30) Leyva, E.; Sagredo, R. *Tetrahedron* **1998**, *54*, 7367.

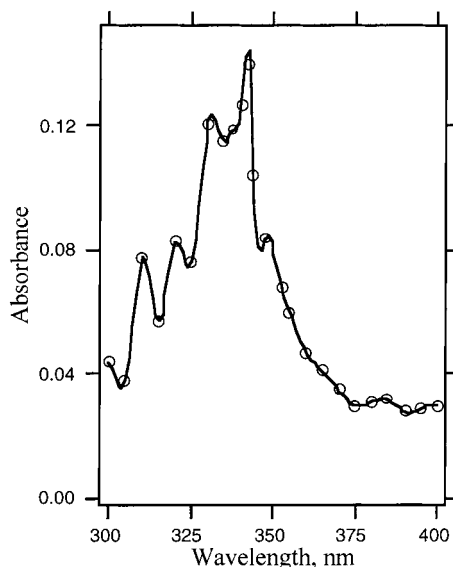
(31) Sundberg, R. J.; Suter, S. R.; Brenner, M. *J. Am. Chem. Soc.* **1972**, *94*, 513.

(32) (a) Reed, A. E.; Weinstock, R. B.; Weinhold, F. A. *J. Chem. Phys.* **1985**, *83*, 735. (b) Reed, A. E.; Weinhold, F. A.; Curtiss, L. A. *Chem. Rev.* **1988**, *88*, 899.

(33) Gritsan, N. P.; Gudmundsdóttir, A. D.; Tigelaar, D.; Platz, M. S. *J. Phys. Chem. A* **1999**, *103*, 3458.

**Table 1.** Spectroscopic and Kinetic Parameters of Some Simple Singlet Arylnitrenes

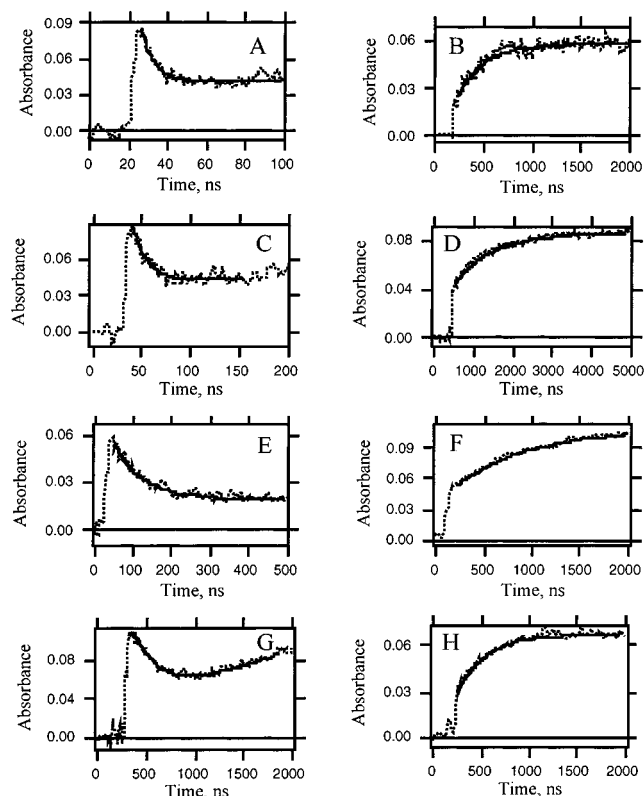
singlet nitrene	$\lambda_{\max}$	$k_{\text{ISC}} (\times 10^6)$	$\tau_{298}$ (ns)	$\log A$ ( $\text{s}^{-1}$ )	$E_a$ (kcal/mol)	solvent
phenyl ( <b>2a</b> ) <sup>8</sup>	350	$3.2 \pm 0.3$	$\sim 1$	$13.1 \pm 0.3$	$5.6 \pm 0.3$	$\text{C}_5\text{H}_{12}$
2-fluorophenyl ( <b>2b</b> )	342	$3.3 \pm 0.5$	$8 \pm 1$	$13.0 \pm 0.3$	$6.7 \pm 0.3$	$\text{C}_5\text{H}_{12}$
	344	—	$10 \pm 2$			$\text{CH}_2\text{Cl}_2$
	344	—	$10 \pm 2$			$\text{CF}_2\text{ClCFCl}_2$
	365	$3.5 \pm 1.4$	$\sim 0.3$	$13.2 \pm 0.3$	$5.3 \pm 0.3$	$\text{C}_5\text{H}_{12}$
4-fluorophenyl ( <b>2c</b> ) <sup>30</sup>	365	$3.5 \pm 1.4$	$\sim 0.3$	$13.2 \pm 0.3$	$5.3 \pm 0.3$	$\text{C}_5\text{H}_{12}$
3,5-difluorophenyl ( <b>2d</b> )	300	$3.1 \pm 1.5$	$\sim 3$	$12.8 \pm 0.3$	$5.5 \pm 0.3$	$\text{C}_5\text{H}_{12}$
2,6-difluoro-phenyl ( <b>2e</b> )	342	$2.4 \pm 0.3$	$240 \pm 20$	$11.5 \pm 0.5$	$7.3 \pm 0.7$	$\text{C}_6\text{H}_{14}$
		$2.7 \pm 0.3$	$260 \pm 20$	$12.0 \pm 1.2$	$8.0 \pm 1.5$	$\text{CCl}_4$
		$3.3 \pm 1.5$	$56 \pm 4$	$12.8 \pm 0.6$	$7.8 \pm 0.6$	$\text{C}_5\text{H}_{12}$
2,3,4,5,6-pentafluoro-phenyl ( <b>2f</b> ) <sup>26</sup>	330	$3.3 \pm 1.5$	$56 \pm 4$	$12.8 \pm 0.6$	$7.8 \pm 0.6$	$\text{C}_5\text{H}_{12}$
		$10.5 \pm 0.5$	$32 \pm 3$	$13.8 \pm 0.3$	$8.8 \pm 0.4$	$\text{CH}_2\text{Cl}_2$

**Figure 5.** The transient absorption spectrum of singlet 2-fluorophenyl nitrene **2b**, recorded point-by-point, after LFP (266 nm) of 2-fluorophenyl azide **1b**. The spectrum was recorded in pentane at 295 K 2 ns after the laser pulse.

nitrene **2b** and azirine **3b** interconvert under the experimental conditions (Schemes 3 and 4).

This hypothesis is supported by the spectroscopic data. Figure 8 (spectrum 1) presents the spectrum of the products formed from the decay of singlet nitrene **2b** at room temperature. This spectrum is the sum of the spectrum of triplet nitrene **6b** (narrow band at 303 nm and weak absorption below 450 nm) and ketenimine **4b** (broad band at 350 nm). We can compare this complicated spectrum with the simpler spectrum of ketenimine **4c** detected after LFP of azide **1c** (spectrum 2) and the spectrum of triplet nitrene **6b** observed as a persistent species in a low-temperature matrix (spectrum 3). According to this result the yield of triplet nitrene **6b** is significant at room temperature. However, if one postulates that azirine **3b** does not interconvert with singlet nitrene **2b** (Scheme 1,  $k_E \gg k_{-R}$ ), then the yield of triplet nitrene at room temperature should be very small and equal to  $k_{\text{ISC}}/k_{\text{OBS}} \approx 0.03$ , where  $k_{\text{OBS}}$  is the observed pseudo-first-order rate constant for the disappearance of singlet nitrene **2b**. Nevertheless, spectrum 1 of Figure 8 has a large contribution of the spectrum of triplet nitrene **6b**. This can be explained if benzazirine **3b** serves as a reservoir for singlet 2-fluorophenyl nitrene **2b** (at temperatures higher than 180 K), which eventually relaxes to triplet nitrene **6b**.

It is known that certain cyclic ketenimines revert slowly to singlet aryl nitrenes, but this process occurs on the millisecond time scale.<sup>5</sup> Rearrangement of **2b** occurs on a time scale less than a few microseconds. Therefore, we analyzed our data according to Scheme 4.

**Figure 6.** Changes in transient absorption produced by LFP (266 nm) of **1b** at 342 nm (A, C, E, G) and 380 nm (B, D, F, H) at selected temperatures: 295 K (A, B), 273 K (C, D), 233 K (E, F), and 160 K (G, H).

The system of differential equations describing the time dependence of the concentrations of **2b**, **3b**, **4b**, and **6b** (Scheme 4) has an analytical solution (Supporting Information). Scheme 4 is a simplification of the complete reaction mechanism which ignores the slow dimerization of triplet nitrene **6b**, the slow polymerization of ketenimine **4b** and its slow reversion to azirine. According to the analytical solution, the time dependencies of the concentrations of all intermediates (**2b**, **3b**, **4b**, and **6b**) can be described by two exponential functions with the same exponents for all intermediates ( $k_1$  and  $k_2$ ). Values of  $k_1$  and  $k_2$  are very complicated nonlinear functions of  $k_R$ ,  $k_{-R}$ ,  $k_{\text{ISC}}$ , and  $k_E$  (Supporting Information). When  $k_1$  and  $k_2$  are significantly different ( $\geq 10$  times), the experimental growth and decay curves can be fit to singlet exponential functions, and  $k_1$  can be assigned to  $k_{\text{dec}}$  and  $k_2$  to  $k_{\text{gr}}$ .

When the temperature is very low, one of the exponents ( $k_2$ ) goes to zero, and the second exponent ( $k_1$ ) becomes equal to  $k_{\text{ISC}}$ . In this situation the singlet nitrene undergoes only one reaction—intersystem crossing to the triplet ground state. Indeed at low temperature ( $\leq 180$  K)  $k_{\text{dec}}$  becomes equal to  $k_{\text{gr}}$ , and

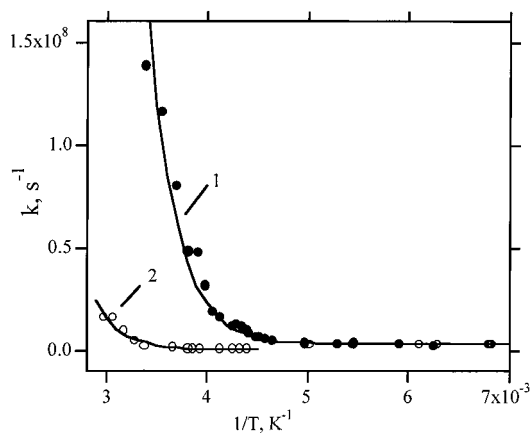


**Figure 7.** The temperature dependences of (1) the rate constant of decay of singlet 2-fluorophenylnitrene **2b** ( $k_{\text{dec}}$ ) and (2) the apparent rate constant ( $k_{\text{gr}}$ ) of formation of triplet 2-fluorophenylnitrene (**6b**) and ketenimine (**4b**). Solid lines 1 and 2: results of nonlinear global fit of the data to analytical solutions.

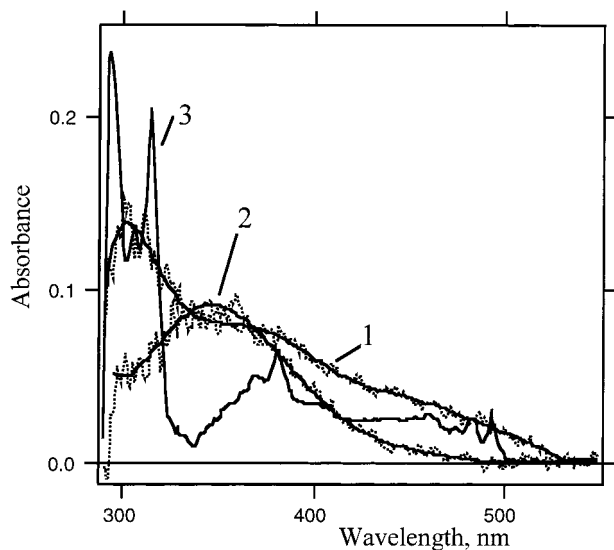
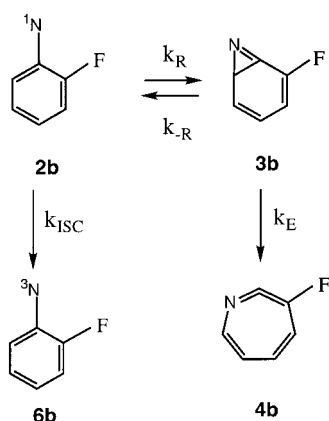


**Figure 8.** Transient absorption spectra produced by LFP (249 nm) at 295 K (1) of 2-fluorophenyl azide **1b** in pentane, detected 500 ns after the laser pulse and (2) 4-fluorophenyl azide **1c** detected 50 ns after the laser pulse and (3) persistent spectrum detected after 20 s of photolysis of **1b** in methylcyclohexane at 77 K.

#### Scheme 4



both are very close to  $k_{\text{ISC}}$  for singlet phenylnitrene<sup>8</sup> and other fluoro-substituted phenylnitrenes (Table 1).

When  $k_{\text{R}}$  and  $k_{-\text{R}}$  are significantly larger than  $k_{\text{ISC}}$  and  $k_{\text{E}}$ , then singlet nitrene **2b** and benzazirine **3b** are in equilibrium

and eventually decay to the lower-energy triplet nitrene **6b** and ketenimine **4b**. In this case the observed rate constants ( $k_{\text{dec}}$  and  $k_{\text{gr}}$ ) can be written in the following simple forms (Supporting Information):

$$k_{\text{dec}} = k_{\text{R}} + k_{-\text{R}} + \frac{k_{\text{ISC}}}{1 + K_{\text{R}}} + \frac{k_{\text{E}}k_{\text{R}}}{1 + K_{\text{R}}} \quad (1)$$

$$k_{\text{gr}} = \frac{k_{\text{ISC}}K_{\text{R}}}{1 + K_{\text{R}}} + \frac{k_{\text{E}}}{1 + K_{\text{R}}} \quad (2)$$

where  $K_{\text{R}} = k_{-\text{R}}/k_{\text{R}}$  is the equilibrium constant for the reverse of the cyclization reaction.

An additional assumption can be made on the basis of the very special temperature dependence of  $k_{\text{gr}}$  (Figure 7). This rate constant changes dramatically when the temperature decreases, but in the 260–220 K temperature range, it becomes practically independent of temperature and reaches a limiting value that is about 3 times smaller than  $k_{\text{ISC}}$ . In this temperature range conversion of **3b** to ketenimine **4b** becomes very slow, the second term in eq 2 can be neglected, and a simplified eq 2a is obtained.

$$k_{\text{gr}} \cong \frac{k_{\text{ISC}}K_{\text{R}}}{1 + K_{\text{R}}} \quad (2a)$$

Using expression 2a and the data of Figure 7, we can estimate the equilibrium constant  $K_{\text{R}}$  as 0.5 at these temperatures. If we assume that  $K_{\text{R}}$  is temperature-dependent in the usual form, then  $K_{\text{R}} = \exp(-\Delta G/RT)$ , and we can estimate  $\Delta G$  as  $\sim 350$  cal/mol. Thus, **2b** and **3b** are very close in energy. Using eq 2 and values of  $k_{\text{ISC}} = 3.3 \times 10^6 \text{ s}^{-1}$  and  $K_{\text{R}} = \exp(-175/T)$ , we extracted the rate constant  $k_{\text{E}}$  and calculated the following Arrhenius parameters (Figure 4, line 5):  $A = 10^{13.5 \pm 0.4} \text{ s}^{-1}$  and  $E_{\text{a}} = 9000 \pm 500$  cal/mol.

Knowing  $k_{\text{ISC}}$ ,  $K_{\text{R}}$  and  $k_{\text{E}}$  allowed us to calculate values of  $k_{\text{R}}$  at temperatures higher than 270 K using eq 1. An Arrhenius treatment of  $k_{\text{R}}$  calculated by this procedure is presented in Figure 4 (line 3). The activation energy for reaction of cyclization of **2b** ( $6700 \pm 300$  cal/mol) is about 1 kcal/mol higher than that for cyclization of parent phenylnitrene ( $5600 \pm 300$  cal/mol).<sup>8</sup>

We also performed a global fitting of the data of Figure 7 to the analytical solution for  $k_1$  and  $k_2$  with  $k_{\text{ISC}} = 3.3 \times 10^6 \text{ s}^{-1}$  and  $K_{\text{R}} = 0.5$ , and with the preexponential factors and activation energies of  $k_{\text{R}}$  and  $k_{\text{E}}$  being adjustable parameters. The results of the best fit are shown in Figure 7 as solid lines (1 and 2). The deduced values of the preexponential factors and activation energies for  $k_{\text{R}}$  and  $k_{\text{E}}$  are very close to the results of our previous analysis (Figure 4, Table 1).

According to the analytical solutions (Supporting Information) for the concentrations of intermediates (Scheme 4), the yield of triplet nitrene ( $\eta$ ) at ambient temperature is given in eq 3

$$\eta = \frac{k_{\text{ISC}}(k_{-\text{R}} + k_{\text{E}})}{k_{\text{ISC}}k_{\text{E}} + k_{\text{R}}k_{\text{E}} + k_{\text{ISC}}k_{-\text{R}}} \cong \frac{1}{1 + k_{\text{R}}k_{\text{E}}/k_{\text{ISC}}k_{-\text{R}}} = 0.2 \quad (3)$$

This result is consistent with the transient spectrum of Figure 8 (spectrum 1). Note that the total yield of azo compound product derived from triplet nitrene **6b** could be higher than 20% due to the slow reversion of ketenimine **4b** on the millisecond time scale.

**Azo Compound Formation.** Photolysis of phenyl azide produces singlet phenylnitrene **2a** which can cyclize to an azirine

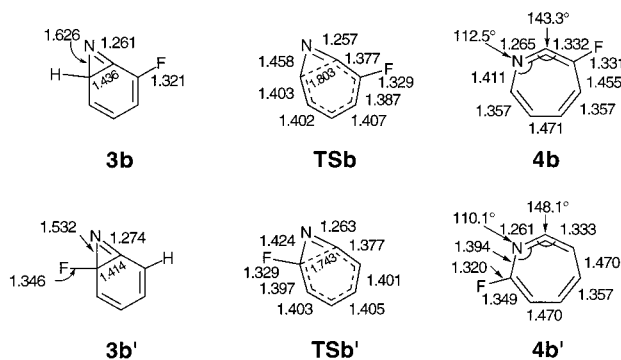


**Figure 9.** Selected CASSCF(8,8)/6-31G\* optimized geometric parameters of stationary points involved in the electrocyclic ring opening of bicyclic azirines **3b** and **3b'**. Distances in Å, angles in degrees.

**3a** which subsequently opens to ketenimine **4a** (Scheme 1) or undergoes intersystem crossing to form triplet phenylnitrene **6a** which will dimerize to form azobenzene **7a**. Under conditions of low dilution the ketenimines will polymerize faster than they will revert to azirine and singlet nitrene.<sup>2,5</sup> Thus, when azirine formation is irreversible, the yield of azo compound derived from a simple aryl azide will be  $k_{ISC}/(k_{ISC} + k_R) \times 100\%$ . At 298 K this model predicts that the yield of azo compound obtained upon photolysis of 4-fluorophenyl azide **1c** and 2,6-difluorophenyl azide **1e** in pentane at 298 K should be 0.3% and 62%, respectively. Upon photolysis of **1c** and **1e** yields of 2 and 23% were observed, respectively. The lower than expected yield of azo dimer **7e** can be explained by reaction of ketenimine **4e** with azide precursor **1e**, a process known in the parent system,<sup>2,5</sup> and by insertion of singlet nitrene **2e** into C–H bonds of the solvent.<sup>12</sup>

Photolysis of 2-fluorophenyl azide **1b** at 298 K in pentane is predicted to give a maximum yield of azo compound **7b** of 3% if azirine and ketenimine formation is irreversible. Nevertheless, photolysis of 2-fluorophenyl azide **1b** in pentane at 298 K gives a 76% yield of azo compound (and triplet nitrene) is consistent with our conclusion that azirine **3b**, ketenimine **4b**, and singlet nitrene **2b** interconvert, leading to an enhanced yield of triplet nitrene. The yield of **7b** is much higher than the value estimated according to eq 3. This means that ketenimine **4b** reverts to azirine and singlet nitrene faster than it polymerizes under our experimental conditions.

**Quantum Chemical Calculations.** To aid in understanding the experimental results for nitrenes **2b–2e** and to support our explanation of the unique kinetics for **2b**, we performed a series of ab initio and density functional theory (DFT) calculations on the second step of the ring expansion, that is, the electrocyclic ring opening of azirines **3b–3e** to form the corresponding cyclic ketenimines **4b–4e**. When combined with the earlier results of Karney and Borden on the first step,<sup>22</sup> these results provide an overall view of the energetics of the ring expansion process for fluorinated aryl nitrenes. Representative CASSCF(8,8)/6-31G\* optimized geometries are presented in Figure 9, and the CASPT2/cc-pVDZ//CASSCF(8,8)/6-31G\* and B3LYP/6-31G\* energies are given in Table 2. The CASPT2 results are also depicted graphically in Figure 10, in a way that permits energetic comparisons of isomeric species. Of the two possible modes of ring expansion for nitrene **2b**, “away” ring expansion refers to that arising via initial cyclization of nitrogen *away* from the carbon bearing fluorine (to form **3b** and **4b**), and “toward” refers to that arising via cyclization *toward* the carbon bearing fluorine (to form **3b'** and **4b'**).

The CASSCF(8,8)/6-31G\* geometries of azirines **3b** and **3b'**, cyclic ketenimines **4b** and **4b'**, and the corresponding transition

states for ring opening (**TSb** and **TSb'**) are provided in Figure 9. These two systems represent the two extremes with regard to several geometric features. The computed geometry of azirine **3b** is very similar to that of azirine **3a**, at the same level of theory.<sup>25</sup> In contrast, the C–F and C=N bond lengths in **3b'** (1.346 and 1.274 Å, respectively) are predicted to be significantly longer than those in **3b** (1.321 and 1.261 Å), due to a filled–unfilled orbital interaction between the C=N  $\pi$  MO and the low-lying C–F  $\sigma^*$  orbital.<sup>22</sup> This interaction also results in significantly shorter C–N and C–C single bonds in the azirine ring of **3b'** compared to **3b**, and is perhaps partly responsible for the greater stability of **3b'** relative to **3b** and **3c**. (see Figure 10).

The differences in C–N and C–C single-bond lengths in **3b'** relative to **3b** are propagated to the corresponding transition states. Most noticeable is the difference in computed lengths of the breaking C–C bond: 1.743 Å in **TSb'**, versus 1.803 Å in **TSb**. For comparison, the corresponding distance in the parent system (**TSa**) is predicted to be 1.778 Å. The longer C–C distance in **TSb** compared to parent **TSa** is most likely due to a filled–unfilled orbital interaction between the high-lying C–C  $\sigma$  MO and the low-lying C–F  $\sigma^*$  orbital, since these two bonds are in a roughly antiperiplanar arrangement.

The most noticeable difference in the geometries of the two ketenimines **4b** and **4b'** is the smaller N=C=C angle in **4b** (143.3°) as compared to **4b'** (148.1°). The angle in **4b'** is very similar to that in **4a** (148.3°). The smaller angle in **4b** facilitates overlap between the empty C–F  $\alpha^*$  MO and the back lobe of the lone-pair orbital on nitrogen.

As shown in Figure 10, in all cases except the “away” ring expansion of 2-fluorophenyl nitrene (**2b**), the transition state for the second step of the ring expansion (**3**  $\rightarrow$  **4**) is computed to be lower in energy than that for the first step (**2**  $\rightarrow$  **3**) at the CASPT2 level of theory. This is consistent with the experimental finding that, for nitrenes **2c–2e**, the nitrene decays at the same rate at which the corresponding ketenimine is formed, whereas for nitrene **2b**, nitrene decay is faster than ketenimine growth. In addition, of the five electrocyclic ring openings studied here, the opening of **3b** to form **4b** is predicted to be the least exothermic ( $\Delta E = -1.6$  kcal/mol). The exothermicity of this step for the other systems ranges from  $\Delta E = -2.7$  kcal/mol for **3d**  $\rightarrow$  **4d**, to  $\Delta E = -6.0$  kcal/mol for **3b'**  $\rightarrow$  **4b'**.

The CASPT2 results are supported qualitatively by B3LYP/6-31G\* calculations, the results of which are shown in Figure 11. All of the benzazirines are given the same relative energy, which for convenience is set to zero. The DFT calculations predict that benzazirine **3b** has the second-highest barrier (after **3f**) to rearrangement to a ketenimine. It also has the lowest barrier to reversion to the corresponding singlet nitrene (**2b**)<sup>22</sup> (Figure 10). Thus, **3b** reverts to the corresponding singlet nitrene more readily than does the parent system **3a**. The DFT calculations also predict that, of the four systems studied experimentally in this work, the ring opening **3b**  $\rightarrow$  **4b** is the least exothermic. Thus, both CASPT2 and B3LYP calculations correctly predict that **3b** is the benzazirine most likely to revert to the corresponding singlet nitrene. Significantly, this is the only system of the four studied in this work in which the rates of formation and disappearance of the benzazirine are predicted to be comparable, and the only case where there is compelling kinetic evidence in favor of an intermediate between the singlet nitrene and its ketenimine isomer in solution.

The experimental data reveal that singlet nitrene **2b** and benzazirine **3b** are very close in energy ( $\Delta G \approx 350$  cal/mol). This value is smaller than that predicted by CASPT2 calculations

**Table 2.** Relative Energies (in kcal/mol) and Zero-Point Vibrational Energies of Azirines **3**, Ketenimines **4**, and the Transition States (TS) Connecting Them<sup>a</sup>

method	azirine		transition state		ketenimine	
	<i>E</i>	ZPE	rel <i>E</i>	ZPE	rel <i>E</i>	ZPE
	<b>3a</b>		<b>TSa</b>		<b>4a</b>	
CASPT2/cc-pVDZ <sup>b</sup>	-285.41815	60.9	2.5	59.8	-4.5	60.8
B3LYP/6-31G* <sup>c</sup>	-286.27659	57.7	4.7	56.7	-5.1	57.6
	<b>3b</b>		<b>TSb</b>		<b>4b</b>	
CASPT2/cc-pVDZ <sup>b</sup>	-384.47462	55.7	7.0	54.6	-1.6	55.8
B3LYP/6-31G* <sup>c</sup>	-385.50238	52.8	8.1	51.7	-3.0	52.8
B3LYP/6-311+G(2d,p) <sup>c</sup>	-385.62115		7.0		-5.4	
CCSD(T)/6-31+G* <sup>c</sup>	-384.48202		11.2			
	<b>3b'</b>		<b>TSb'</b>		<b>4b'</b>	
CASPT2/cc-pVDZ <sup>b</sup>	-384.48308	55.9	2.4	54.8	-6.0	55.7
B3LYP/6-31G* <sup>c</sup>	-385.51174	52.7	4.1	51.8	-6.8	52.8
	<b>3c</b>		<b>TSc</b>		<b>4c</b>	
CASPT2/cc-pVDZ <sup>b</sup>	-384.48077	55.6	4.5	54.5	-4.3	55.5
B3LYP/6-31G* <sup>c</sup>	-385.50865	52.6	5.7	51.5	-5.5	52.6
	<b>3d</b>		<b>TSd</b>		<b>4d</b>	
CASPT2/cc-pVDZ <sup>b</sup>	-483.52115	50.5	5.2	49.3	-2.7	50.3
B3LYP/6-31G* <sup>c</sup>	-484.74392	47.7	6.4	46.6	-3.9	47.6
	<b>3e</b>		<b>TSe</b>		<b>4e</b>	
CASPT2/cc-pVDZ <sup>b</sup>	-483.51566	50.7	5.7	49.6	-3.7	50.6
B3LYP/6-31G* <sup>c</sup>	-484.73747	47.8	6.7	46.8	-5.1	47.9
B3LYP/6-311+G(2d,p) <sup>c</sup>	-484.89484		6.4		-6.5	
	<b>3f</b>		<b>TSf</b>		<b>4f</b>	
B3LYP/6-31G* <sup>c</sup>	-782.41002	32.6	8.5	31.5	-6.0	32.6

<sup>a</sup> Azirine energies are absolute energies, in hartrees. Energies for transition states and ketenimines are relative energies, compared to the azirines.

<sup>b</sup> Obtained using CASSCF(8,8)/6-31G\* optimized geometry. Relative energies are corrected for differences in zero-point vibrational energy. <sup>c</sup> Obtained using B3LYP/6-31G\* optimized geometry. Relative energies are not corrected for differences in zero-point vibrational energy.

(4.8 kcal/mol, Figure 8). The CASPT2 method typically underestimates by 3–6 kcal/mol<sup>22</sup> the energies of open-shell species, such as **2b**, relative to those of closed-shell molecules, such as **3b**.<sup>29</sup> Applying an upward correction of 2–3 kcal/mol to the energy of the singlet nitrene as in the case of **2a** brings the computational result into much better agreement with experiment.

### III. Discussion

A *para*-fluorine substituent has no effect, outside of experimental error, on the barrier to cyclization of a singlet phenylnitrene. The electronic effect via  $\pi$ -back-bonding of the lone pair of electrons of the fluorine substituent is negligible. Furthermore, placement of two fluorine substituents in the *meta* positions does not influence the barrier to cyclization of the nitrene. There is no long-range inductive effect of fluorine on the rate of cyclization. Indeed, according to the predictions of theory,<sup>22,25</sup> the cyclization of singlet aryl nitrenes involves what may be regarded as an intramolecular coupling reaction of two initially orthogonal radical centers. Thus, large *para* or *meta* substituent effects on this reaction are not expected.

Singlet 2,6-difluorophenylnitrene (**2e**) and singlet perfluorophenylnitrene (**2f**) react with hydrocarbon solvents by insertion into C–H bonds.<sup>12</sup> In the case of nitrenes **2e** and **2f** in hydrocarbon solvent,  $k_{\text{OBS}}$  is actually

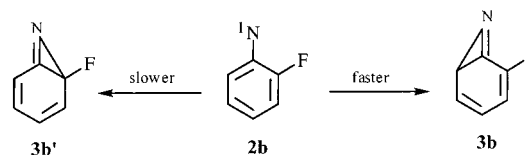
$$k_{\text{OBS}} = k_{\text{ISC}} + k_{\text{R}} + k_{\text{SH}}[\text{SH}]$$

where the latter term reflects the contribution of the reaction of the singlet nitrene with solvent. In these cases, the slope of a plot of  $\log(k_{\text{OBS}} - k_{\text{ISC}})$  versus  $1/T$  is not simply related to the

barrier to cyclization. Thus, values of  $E_{\text{a}}$  in hydrocarbon solvents are smaller than those measured in the less reactive solvents  $\text{CH}_2\text{Cl}_2$ ,  $\text{CCl}_4$ , and  $\text{CF}_2\text{ClCFCl}_2$  (Table 1). On the basis of product studies we are confident that the activation energy barriers determined in the latter solvents can be associated with the cyclization of the singlet nitrene.<sup>12</sup>

Placement of fluorine substituents at both *ortho* positions raises the barrier to cyclization by about 3 kcal/mol, relative to the unsubstituted system (Table 1). One can worry, of course, that compensating experimental errors in the activation energies and preexponential terms may obscure or falsely amplify trends in the barrier heights. For this reason it is useful to compare singlet aryl nitrene lifetimes at 298 K, which are controlled by cyclization. The lifetimes of singlet phenylnitrene (**2a**) and 4-fluorophenylnitrene (**2c**) are about 1 ns or less at 298K. The lifetime of 3,5-difluorophenylnitrene (**2d**) is about 3 ns at 298 K but that of 2,6-difluorophenylnitrene (**2e**) is 260 ns, in  $\text{CCl}_4$ . As a *para*-fluoro group fails to exert an electronic influence on the cyclization process, it is tempting to attribute the effect of two *ortho*-fluorine substituents on the singlet nitrene lifetime to a simple steric effect.

This interpretation is consistent with the calculations of Karney and Borden, who found that cyclization *away* from an *ortho*-methyl or an *ortho*-fluorine group is favored by 2–3 kcal/mol relative to cyclization *toward* the substituent.<sup>22</sup>





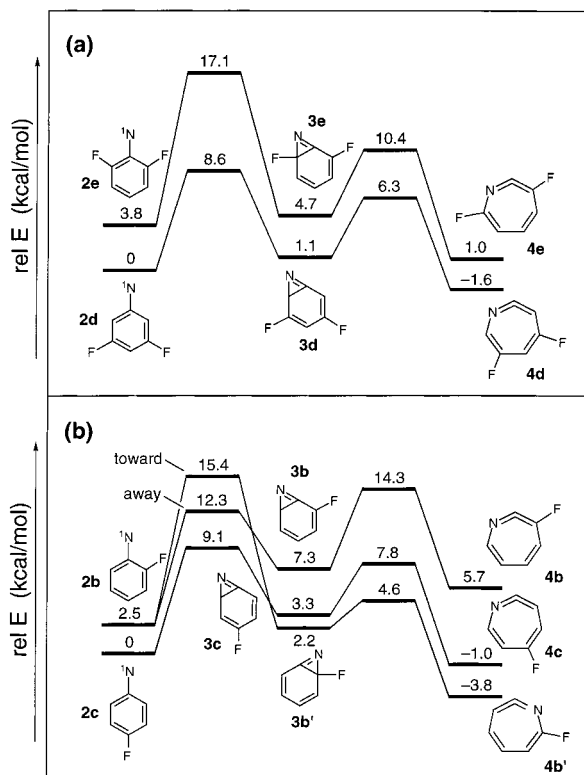


**Figure 10.** Relative energies (in kcal/mol) of species involved in the ring expansions of singlet fluoro-substituted phenylnitrenes calculated at the CASPT2/cc-pVDZ//CASSCF(8,8)/6-31G\* level. (a) Difluorinated phenylnitrenes. (b) Monofluorinated phenylnitrenes. Data for the first step (2 → 3) taken from ref 22.

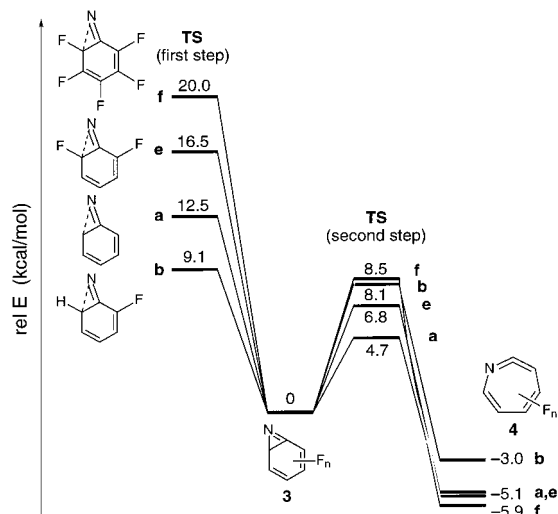
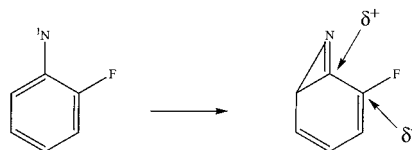


**Figure 11.** Relative energies (in kcal/mol) of species involved in the ring expansions of singlet fluoro-substituted phenylnitrenes calculated at the B3LYP/6-31G\* level of theory (where a, b, e, f are as described in Scheme 2).

The work of Leyva, et al. demonstrated, in fact, that cyclization of the singlet nitrene **2b** proceeds away from the fluorine substituent.<sup>30</sup> Sundberg et al. demonstrated this same pattern much earlier with *ortho*-alkyl substituents.<sup>31</sup> Our results are in good quantitative agreement with the computational data of Karney and Borden,<sup>22</sup> who predicted that the barrier to cyclization of **2b** away from the fluorine substituent will be about 1 kcal/mol higher than that for parent system **2a**. The experimental difference is the same (Table 1).

The steric argument predicts that a single *ortho*-fluorine substituent will have little influence on the rate of conversion of **2b** to **3b**, since cyclization occurs at the unsubstituted *ortho* carbon. However, the barrier to this process is larger (outside of experimental error) than that of the parent system. In fact, the lifetime of singlet 2-fluorophenylnitrene (**2b**) at 298 K is 8–10 times longer than that of the parent (**2a**) and 20–30 times longer than that of 4-fluorophenylnitrene (**2c**). Therefore, a single *ortho*-fluorine atom exerts a small but significant bystander effect on remote cyclization that is not simply steric in origin.

To understand this substituent effect, we have computed the atomic charges for the different centers using the CASSCF(8,8)/6-31G\* wave functions and the natural population analysis (NPA) method of Reed and Weinhold.<sup>32</sup> The results are shown in Figure 12 for formation of the azirines derived from 4-fluoro- (**2c** → **3c**) and from 2-fluorophenylnitrene (**2b** → **3b** and **2b** → **3b'**). The most important values for discussion have been marked in bold in Figure 12 for clarity. For the parent nitrenes, fluorine substitution in **2b** and **2c** makes the adjacent carbon very positively charged; according to the NPA results, the C bearing F has a charge of about +0.48 e. In **2b**, the *ortho* carbon to the C–N fragment has a –0.20 atomic charge if F is not also attached. For 4-fluorophenylnitrene (**2c**), transformation from **2c** to **TS2c**–**3c** shows an increase in positive character at the (*ipso*) carbon bearing the nitrogen (from 0.08 to 0.12 e); furthermore, the C at the site of insertion for the forming C–N bond also becomes more positive (–0.20 to –0.17 e). In the transformation of 2-fluorophenylnitrene (**2b**) to **TS2b**–**3b** (away from F) or **TS2b**–**3b'** (toward F), there is a similar increase in positive charge at the carbon which bears the nitrogen. The significant effects are at the *ortho* carbons. In **TS2b**–**3b**, the *ortho* carbon where the C···N bond is forming bears a –0.17 atomic charge, and there is a +0.08 atomic charge at the *ipso* carbon (relative to N). The +0.08 charge at the *ipso* carbon is adjacent to the +0.47 charge at the carbon adjacent to F, and this leads to the increase in activation barrier for 2-fluorophenylnitrene relative to 4-fluorophenylnitrene even when nitrogen insertion occurs away from the fluorine substituent in **TS2b**–**3b**. For insertion toward F in **TS2b**–**3b'**, the situation is even worse. There is even greater amount of +····+ interaction between the *ortho* (+0.49 e) and *ipso* (+0.08 e) carbons in **TS2b**–**3b'**, and this leads to a higher activation barrier for insertion toward F than away from F.



This leads to increased positive-positive charge repulsion in the transition state leading to the benzazirine and raises the barrier to cyclization.

**Reversible Intramolecular Reactions.** Previous workers have postulated that singlet aryl nitrenes and ketenimines interconvert.<sup>5</sup> Our work with singlet 2-fluorophenylnitrene requires that there be an intermediate in the transformation of **2b** to **4b** in solution. It is most reasonable to associate this intermediate with benzazirine **3b**. This conclusion may be generally true throughout the series of compounds studied previously<sup>23,33,34</sup> and in this work, but compelling *kinetic* data are available only with singlet nitrene **2b**. Triplet nitrene **6b** is also formed more

(34) Gritsan, N. P.; Tigelaar, D.; Platz, M. S. *J. Phys. Chem. A* **1999**, *103*, 4465.

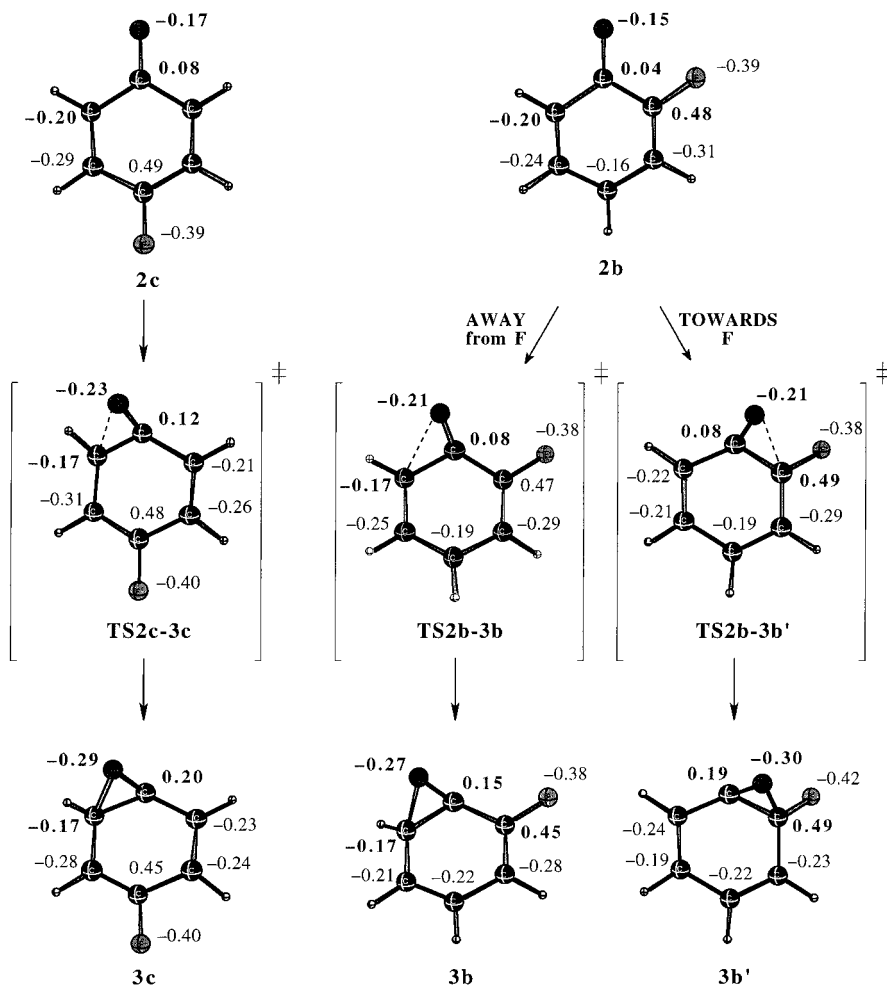
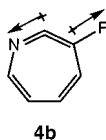


**Figure 12.** NPA atomic charges for the minima and transition states for azirine formation from 2-fluoro- and 4-fluorophenyl nitrenes (**2b** and **2c**, respectively).

slowly than the decay of singlet nitrene **2b**. This observation requires that the singlet nitrene is in equilibrium with benzazirine **3b**.

The barrier for ring opening of **3b** to **4b** was calculated at different levels of theory and falls into the range 7–11.2 kcal/mol (Table 2). This result is in quantitative agreement with the activation energy ( $9000 \pm 500$  cal/mol) of the electrocyclic ring-opening reaction of azirine **3b** (Figure 4, line 5).

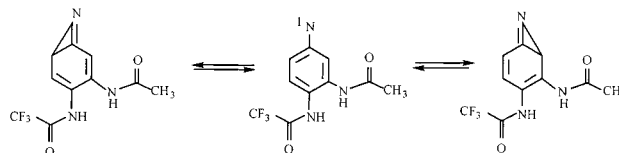
Why is the barrier for ring opening of **3b** to **4b** so much higher than the corresponding barriers for **3a** and **3c–3e**? As shown in Figures 10 and 11, for all cases except **3f**  $\rightarrow$  **4f**, the energy of the transition state for this step roughly parallels the energy of the ketenimine product. The marked instability of ketenimine **4b**, relative to that of **4b'** and **4c**, is consistent with recent computational results predicting that fluorine substitution destabilizes ketenimines.<sup>35</sup> This instability can be attributed to Coulombic repulsion between the two carbons of the ketenimine moiety. Because both of these carbons are attached to more electronegative atoms (one to N, one to F), both bear a partial positive charge as shown below, and repulsion would result.



On the other hand, a fluorine adjacent to the nitrogen in a ketenimine is stabilizing, as in **4b'**, presumably due to partial

delocalization of the nitrogen lone pair into the C–F  $\sigma^*$  orbital. The effect of Coulombic repulsion described for ketenimine **4b** can also be used to rationalize the higher energy of azirine **3b** relative to that of **3b'** and **3c**. It is possible that the changes in relative orientation of the C=N and C–F bond dipoles that occur for **2b**  $\rightarrow$  **3b** and **3b**  $\rightarrow$  **4b** are at least partly responsible for the fact that this process is predicted to be substantially more endothermic (in the case of **2b**  $\rightarrow$  **3b**) or less exothermic (in the case of **3b**  $\rightarrow$  **4b**) than the other systems studied.

Significantly, **2b**  $\rightarrow$  **3b**  $\rightarrow$  **4b** is the only system of the four studied in this work in which the rates of formation and disappearance of the benzazirine are predicted to be comparable, and the only case where there is compelling kinetic evidence in favor of an intermediate between the singlet aryl nitrene and ketenimine isomer in solution. It should be noted, however, that indirect evidence for the interconversion of a singlet aryl nitrene and a benzazirine was obtained by Younger and Bell<sup>5c</sup> for a 3,4-diamido-substituted phenyl nitrene system.



Curiously, the addition of a second *ortho*-fluorine substituent (i.e., in benzazirine **3e**) raises the barrier to reversion to singlet nitrene **2e**, relative to the mono *ortho*-fluoro system<sup>22</sup> (Figure 10). This is partly due to steric hindrance by fluorine in the transition state for cyclization, but also to the stabilization of **3e** by the fluorine attached directly to the azirine ring (vide supra).<sup>22</sup> The addition of a second fluorine (benzazirine **3e**) decreases the barrier to conversion of azirine **3e** to ketenimine **4e** slightly (Figure 10). This is related to the more favorable thermodynamics of conversion in the case of **3e** compared with **3b**, due to the slight stabilization of ketenimine **4e** by the fluorine adjacent to nitrogen. The barrier for **3e** → **4e** is still predicted to be ~2.5 kcal/mol higher than the barrier for **3a** → **4a** at the same level of theory,<sup>25</sup> which helps to explain why Morawietz and Sander observed benzazirine **3e** rather than ketenimine **4e** in their matrix isolation experiments.<sup>27</sup>

The B3LYP/6-31G\* calculations also indicate that perfluorobenzazirine **3f** must surmount the largest barrier (8.5 kcal/mol) to form a ketenimine (Figure 11).<sup>36</sup> This explains why Morawietz and Sander were also able to observe **3f** under matrix isolation conditions.<sup>27</sup>

#### IV. Conclusions

A series of fluoro-substituted aryl azides were studied by laser flash photolysis (LFP, 249 and 266 nm) techniques. LFP produces singlet fluorinated aryl nitrenes which have characteristic sharp absorption bands with maxima between 300 and 365 nm. At ambient temperature the nitrenes decay by cyclization to benzazirines. Barriers to cyclization of 4-fluoro-, 3,5-difluoro-, 2-fluoro-, 2,6-difluoro-, and 2,3,4,5,6-pentafluoro-phenyl nitrene in inert solvents are  $5.3 \pm 0.3$ ,  $5.5 \pm 0.3$ ,  $6.7 \pm 0.3$ ,  $8.0 \pm 1.5$ , and  $8.8 \pm 0.4$  kcal/mol, respectively. The barrier to cyclization of parent singlet phenyl nitrene is  $5.6 \pm 0.3$  kcal/mol.<sup>7</sup> These values are in very good agreement with CASPT2 calculations for the barriers to conversion of fluoro-substituted singlet aryl nitrenes to benzazirines.<sup>22</sup> Two *ortho*-fluorine substituents retard the cyclization dramatically. The *ortho*-difluoro effect is due to a combination of the steric influence of the fluorines and the build-up of positive charge on adjacent carbon atoms. Kinetic evidence is presented that the cyclization of 2-fluorophenyl nitrene to a benzazirine is reversible. The equilibrium has  $\Delta G \approx 350$  cal/mol between 220 and 260 K. Ab initio calculations on a series of benzazirines, their isomeric ketenimines, and the transition states converting the benzazirines to ketenimines give results that are in good qualitative and quantitative agreement with the experimental findings.

#### V. Experimental Section

**Materials.** Azides **1a**–**1e** were prepared by known procedures from the corresponding anilines.<sup>6,37</sup> Azo compounds **7b**, **7c**, and **7e** were prepared by a literature procedure.<sup>38</sup> The azides were characterized with IR, <sup>1</sup>H NMR, and <sup>13</sup>C NMR spectroscopy and the spectra compared with those reported previously in the literature. Alkane solvents were used as received, but methylene chloride and Freon-113 were purified by passage through a column of basic alumina (activity I).

**Azo Compound Formation.** Azides **1b**, **1c**, and **1e** were photolyzed under identical conditions. The procedure for photolysis of 4-fluorophenyl azide **1c** is representative; 0.0531 g of 4-fluorophenyl azide (0.033 M) and 0.078 mL decane (0.04 M) were dissolved in 10.0 mL of spectral grade pentane. 0.5 mL aliquots of the solution (0.033 M)

were then placed in 4 mm Pyrex tubes. The solutions were degassed using 3-freeze–pump–thaw cycles, which were then sealed under vacuum. Samples were photolyzed for 4 h with 350 nm lamps in a Luzchem photoreactor. Product yields were monitored by GC–MS. The corresponding azo compound response factors were found compared to decane. Only trace yields of anilines were observed.

**Apparatus.** A Nd:YAG laser (Continuum PY62C-10, 35 ps, 10 mJ, 266 nm), and Lumonics TE-860-4 excimer laser (KrF, 10 ns, 50 mJ, 249 nm) were used as the excitation light sources. The laser apparatus system at The Ohio State University has previously been described in detail.<sup>26</sup>

A typical solution was contained in a quartz cuvette which was placed in a quartz cryostat. Some samples were purged with argon prior to photolysis, but the presence of oxygen was found to have no effect on the lifetimes of the singlet nitrenes. Temperature was controlled by passing a thermostabilized nitrogen stream and kept to within  $\pm 1$  K. In the Arrhenius plots at least two kinetic traces were obtained at each temperature, and the observed rate of the disappearance of the signal was averaged. The sample solutions were changed after every laser shot to avoid effects due to the accumulation of a photoproduct. Transient spectra were obtained by laser flash photolysis (Nd:YAG laser) of the sample and detection of kinetic traces at a single wavelength, with variation of the wavelength, in increments of 2.5–5 nm from 300 to 600 nm. The absorption spectra of long-lived ( $\tau \geq 300$  ns) intermediates were measured using an excimer KrF laser (Lumonics, 10 ns, 50 mJ, 249 nm) in conjunction with an optical multichannel analyzer (EG & G Princeton Applied Research, model 1460).

**Computational Methods.** Geometry optimizations and transition state searches were performed using the 6-31G\* basis set,<sup>39</sup> in conjunction with either the B3LYP<sup>40</sup> or complete active space SCF (CASSCF) method.<sup>41</sup> The CASSCF calculations used an 8-electron, 8-orbital active space, hereafter designated (8,8), for all species. The eight orbitals included in the active space are analogous to those used in similar calculations on species involved in the ring expansion of phenyl nitrene.<sup>25</sup> For the 2-fluorophenyl nitrene system, geometries were also computed at the MP2/6-31G\* level.<sup>42</sup> The nature of all stationary points (i.e., either minima or transition states) was determined by calculating the vibrational frequencies at either the B3LYP/6-31G\* or CASSCF(8,8)/6-31G\* level, and the unscaled frequencies were used to obtain corrections for zero-point vibrational energies.

Since the CASSCF method accounts only for static electron correlation, the effects of including dynamic electron correlation<sup>42</sup> were determined by CASPT2 calculations<sup>44</sup> using Dunning's correlation-consistent polarized valence double- $\zeta$  basis set (cc-pVDZ),<sup>45</sup> at the CASSCF(8,8)/6-31G\* optimized geometries. Additional single-point energies were calculated at the B3LYP/6-311+G(2d,p)//B3LYP/6-31G\* and CCSD(T)/6-31+G\*//B3LYP/6-31G\* levels.<sup>46</sup>

All calculations were performed using the Gaussian 94<sup>47</sup> and MOLCAS<sup>48</sup> software packages.

**Acknowledgment.** Support of this work by the National Science Foundation is gratefully acknowledged (NSF CHE-9613861 and CHE-9733457). N.P.G. gratefully acknowledges the support of the National Research Council, and the Russia

(39) Hariharan, P. C.; Pople, J. A. *Theor. Chim. Acta* **1973**, *28*, 213.

(40) (a) Becke, A. D. *J. Chem. Phys.* **1993**, *98*, 5648. (b) Lee, C.; Yang, W.; Parr, R. G. *Phys. Rev. B* **1988**, *37*, 785.

(41) (a) Roos, B. O. *Adv. Chem. Phys.* **1987**, *69*, 339. (b) Roos, B. O. *Int. J. Quantum Chem. Symp.* **1980**, *14*, 175.

(42) Moller, C.; Plesset, M. S. *Phys. Rev.* **1934**, *46*, 618.

(43) For a review on the importance of including dynamic correlation, see: Borden, W. T.; Davidson, E. R. *Acc. Chem. Res.* **1996**, *29*, 67.

(44) (a) Andersson, K.; Malmqvist, P.-A.; Roos, B. O.; Sadlej, A. J.; Wolinski, K. *J. Phys. Chem.* **1990**, *94*, 5483. (b) Andersson, K.; Malmqvist, P.-A.; Roos, B. O. *J. Chem. Phys.* **1992**, *96*, 1218.

(45) Dunning, T. H., Jr. *J. Chem. Phys.* **1989**, *90*, 1007.

(46) (a) Cizek, J. *Adv. Chem. Phys.* **1969**, *14*, 35. (b) Purvis, G. D.; Bartlett, R. J. *J. Chem. Phys.* **1982**, *76*, 1910. (c) Gauss, J.; Cremer, C. *Chem. Phys. Lett.* **1988**, *150*, 280. (d) Raghavachari, K.; Trucks, G. W.; Pople, J. A.; Head-Gordon, M. *Chem. Phys. Lett.* **1989**, *157*, 479.

(36) Kozankiewicz, B.; Deperasinska, I.; Zhai, H. B.; Zhu, Z.; Hadad, C. M. *J. Phys. Chem. A* **1999**, *103*, 5003.

(37) (a) Smalley, R. K.; Suschitzky, H. *J. Chem. Soc.* **1964**, 5922. (b) Hashizumi, K.; Hashimoto, N.; Miyake, Y. *J. Org. Chem.* **1995**, *60*, 6680.

(38) Leyva, E.; Munoz, D.; Platz, M. S. *J. Org. Chem.*, **1989**, *54*, 5938.

Foundation for Basic Research (grant N 98-03-32021). W.L.K. thanks the University of San Francisco Faculty Development Fund and the Lily Drake Cancer Research Fund for generous financial support. We gratefully acknowledge useful conversations with Professor Borden of The University of Washington.

---

(47) Frisch, M. J.; Trucks, G. W.; Schlegel, H. B.; Gill, P. M. W.; Johnson, B. G.; Robb, M. A.; Cheeseman, J. R.; Keith, T.; Petersson, G. A.; Montgomery, J. A.; Raghavachari, K.; Al-Lahaam, M. A.; Zakrzewski, V. G.; Ortiz, J. V.; Foresman, J. B.; Cioslowski, J.; Stefanov, B. B.; Nanayakkara, A.; Challacombe, M.; Peng, C. Y.; Ayala, P. Y.; Chen, W.; Wong, M. W.; Andres, J. L.; Replogle, E. X.; Gomperts, R.; Martin, R. L.; Fox, D. J.; Binkley, J. S.; Defrees, D. J.; Baker, J.; Stewart, J. J. P.; Head-Gordon, M.; Gonzalez, C.; Pople, J. A. *Gaussian 94*, revision d.2; Gaussian, Inc.: Pittsburgh, PA, 1995.

**Supporting Information Available:** CASSCF(8,8)/6-31G\* optimized Cartesian coordinates and absolute energies for azirines **3b–3e**, transition states **TSb–TSe**, and ketenimines **4b–4e**, the UV–vis spectrum of the azo dimer of triplet nitrene **6b**, and the complete set of differential equations and their solutions (PDF). This material is available free of charge via the Internet at <http://pubs.acs.org>.

JA9944305

---

(48) Anderson, K.; Blomberg, V. R. A.; Fülcher, M. P.; Kello, V.; Lindh, R.; Malmqvist, P.-A.; Noga, J.; Olsen, J.; Roos, B. O.; Sadlej, A.; Seigbahn, P. E. M.; Urban, M.; Widmark, P.-O. *MOLCAS*, version 3; University of Lund: Sweden, 1994.